Published in final edited form as:

Clin Cancer Res. 2012 November 15; 18(22): 6122–6135. doi:10.1158/1078-0432.CCR-12-0397.

Quantitative Immunofluorescence Reveals the Signature of Active B Cell Receptor Signaling in Diffuse Large B Cell Lymphoma

Agata M. Bogusz[1,4], **Richard H. G. Baxter**[2], **Treeve Currie**[1], **Papiya Sinha**[1], **Aliyah R. Sohani**[3], **Jeffery L. Kutok**[1,5], and **Scott J. Rodig**[1]

[1]Department of Pathology, Brigham and Women's Hospital, Boston, MA 02115

[2]Department of Chemistry, Yale University, New Haven, CT 06511

[3]Department of Pathology, Massachusetts General Hospital, Boston, MA 02114

Abstract

Purpose—B cell receptor (BCR) mediated signaling is important in the pathogenesis of a subset of diffuse large B cell lymphomas (DLBCL) and the BCR-associated kinases SYK and BTK have recently emerged as potential therapeutic targets. We sought to identify a signature of activated BCR signaling in DLBCL to aid the identification of tumors that may be most likely to respond to BCR-pathway inhibition.

Experimental Design—We applied quantitative immunofluorescence (qIF) using antibodies to phosphorylated forms of proximal BCR signaling kinases LYN, SYK and BTK and antibody to BCR-associated transcription factor FOXO1 on BCR-crosslinked formalin-fixed paraffin-embedded (FFPE) DLBCL cell lines as a model system and on two clinical cohorts of FFPE DLBCL specimens (n=154).

Results—A robust signature of active BCR signaling was identified and validated in BCR-crosslinked DLBCL cell lines and in 71/154 (46%) of the primary DLBCL patient specimens. Further analysis of the primary biopsy samples revealed increased nuclear exclusion of FOXO1 among DLBCL with qIF evidence of active BCR signaling compared to those without ($p = 0.004$). Nuclear exclusion of FOXO1 was also detected in a subset of DLBCL without evidence of proximal BCR signaling suggesting that alternative mechanisms for PI3K/AKT activation may mediate FOXO1 subcellular localization in these cases.

Correspondence, Scott J. Rodig (srodig@partners.org) and Jeffery Kutok* (jeff.kutok@infi.com), Brigham and Women's Hospital, Department of Pathology, 75 Francis Street, Boston, MA, 02115.

[4]Current address: Department of Pathology, Yale University School of Medicine, New Haven, CT 06510

[5]Current address: Infinity Pharmaceuticals, Cambridge MA 02139

*Currently Senior Director, Molecular Pathology at Infinity Pharmaceuticals, 780 Memorial Drive Cambridge, MA02139

Conflict-of-interest disclosure: The authors declare no competing financial interests.

Author Contributions

A.M.B., designed research, performed experiments, analyzed data and wrote the paper, R.H.G.B analyzed data and wrote the paper, T.C. and P.S. performed experiments, A.R.S. selected clinical samples and provided new reagents, J.L.K. designed research, analyzed data, selected clinical samples, and helped in writing the paper, S.J.R. designed research, selected clinical samples, analyzed data and helped in writing the paper.

Conclusion—This study establishes the feasibility of detecting BCR activation in primary FFPE biopsy specimens of DLBCL. It lays a foundation for future dissection of signal transduction networks in DLBCL and provides a potential platform for evaluating individual tumors in patients receiving novel therapies targeting the BCR pathway.

Introduction

Diffuse large B cell lymphoma (DLBCL) is the most common type of non-Hodgkin lymphoma, accounting for roughly 40% of all adult lymphoid malignancies and over 80% of aggressive lymphomas (1, 2). DLBCL is heterogeneous in its biology and shows variable response to combination chemotherapy and anti-CD20 regimens. Prognosis is poor in ~50% of cases, indicating the need for more individualized therapeutic approaches targeting specific signaling pathways to further improve patient outcomes (3, 4).

BCR expression and signaling are necessary for mature B cell survival and there is increasing evidence for a critical role in lymphomagenesis (5-9). In B-cells, the BCR signaling network is complex and involves the cross-activation and regulation of many signaling molecules. Stimulation of cell surface immunoglobulin (sIg) can occur by an antigen or occur independently of an exogenous ligand to transmit low-level tonic survival signals(9, 10). Stimulation leads to protein tyrosine kinase (PTK)-mediated phosphorylation of the cytoplasmic immunoreceptor tyrosine-based activation motif (ITAM) on the signaling subunit, a disulfide-linked Igα/Igβ (CD79α/CD79β) heterodimer (10). Initial ITAM phosphorylation following receptor ligation is predominantly mediated by the *Src*-family kinase LYN that promotes subsequent recruitment and activation of the effector kinases SYK and BTK (11). SYK is a key player that couples BCR-mediated signals to downstream signaling pathways, and coordinate activation of LYN, SYK and BTK is required for proper BCR signal transduction (12-14). The limiting step in BTK activation appears to be generation of phosphatidylinositol 3,4,5-triphosphates [PI(3,4,5)P_3] by PI3K, which is activated following BCR engagement (15, 16). The BCR-mediated increase of plasma membrane PI(3,4,5)P_3 also leads to recruitment and activation of the serine-threonine kinase AKT. AKT, in turn, mediates cell survival by phosphorylation of FOXO1 which translocates from the nucleus to the cytoplasm thereby disrupting its interaction with pro-apoptotic transcriptional targets (17, 18). Taken together, the current data indicate an intimate but complex association between the proximal BCR signaling cascade and activation of the downstream PI3K/AKT/FOXO1 signaling pathway that promotes cell survival.

The importance of the BCR and PI3K/AKT signal transduction in neoplasia have been recently highlighted by the discovery of pathologic mutations, deletions, and amplifications in the genes encoding key signaling components in these pathways in a subset of primary diffuse large B cell lymphomas (19, 20). While the overall frequency of primary DLBCL with active BCR signaling remains unknown, evidence from both cell lines and patient specimens suggest a significant fraction may rely on BCR signaling for survival (21-24). Moreover, novel pharmacologic inhibitors of key regulatory components in these signaling pathways have shown success in patients with relapsed and refractory B cell lymphoma in the few clinical trials conducted to date (25-27).

Here we describe a robust protein signature underlying proximal BCR signaling in primary DLBCL patient specimens. This signature can be readily evaluated through the use of quantitative immunofluorescence (qIF) analysis of phosphorylated forms of kinases LYN, SYK, and BTK. To validate this signature, we first assessed the levels of basal and stimulated BCR signaling in a panel of ten DLBCL cell lines. We identified distinct groups that differ in their response to BCR crosslinking sIg and established criteria to identify BCR pathway activation with a high degree of confidence. We extended this approach to patient specimens by performing qIF on two primary DLBCL tissue microarrays (TMA) and observed coordinate phosphorylation of LYN, SYK and BTK in 71/154 (46%) of human DLBCLs *in situ*.

We further sought to analyze the effect of proximal BCR signaling on the downstream target FOXO1 by qIF. We found that the majority of cell lines manifest high, constitutive activation of AKT and cytoplasmic FOXO1 that show a correlative increase upon sIg crosslinking. In contrast, a range of FOXO1 subcellular localizations, from almost entirely nuclear to almost entirely cytoplasmic, was observed among primary DLBCLs *in situ*. Importantly, the degree of cytoplasmic FOXO1 was greater among primary DLBCL with coordinate activation of LYN, SYK, and BTK than those without (p=0.004). These results reveal that a significant proportion of primary DLBCLs manifest robust activation of the proximal BCR signaling network that correlates with activation of the biologically significant downstream target FOXO1. We suggest that qIF provides a framework of assessing the integrity and activity of the BCR pathway in DLBCL biopsy samples that will assist in evaluating patients receiving targeted therapy.

Methods

Cell culture

The DLBCL cell lines SUDHL4 (DHL4), SUDHL6 (DHL6), OCI-LY4 (LY4), OCI-LY7 (LY7), Karpas-422 (K422), Pfeiffer, Toledo, HBL-1, and U2932 were cultured in RPMI 1640 medium (Mediatech, Herndon, VA) supplemented with 10% fetal calf serum (FCS) and 2 mM glutamine. The DLBCL cell line OCI-LY3 (LY3) was cultured in Isocove modified Dulbecco medium (IMDM) (Invitrogen, Grand Island, NY) supplemented with 20% human serum (Gemini Bio-Products, West Sacramento, CA) and 2 mM glutamine. All cells were maintained at 37°C in 5% CO_2. Cells were kindly provided at the time of study by the laboratory of Prof. Margaret Shipp (Dana-Farber Cancer Institute, Boston, MA), and were originally obtained from the following sources: Pfeiffer and Toledo, American Tissue Culture Collection (ATCC, Manasssas, VA); SUDHL4, SUDHL6 and K422, Deutsche Sammlung von Mikroorganismen und Zellkulturen GmbH (DSMZ, Braunschweig, Germany), and OCI-LY3, OCI-LY4 and OCI-LY7, Ontario Cancer Institute (The University of Toronto, Toronto, ON, Canada). Access to HBL-1 and U2932 were provided courtesy of Prof. Georg Lenz (Charité–Universitätsmedizin, Berlin).

The identities of the DLBCL cell lines used in this study were confirmed via STR profiling (PowerPlex® 1.2 system, Promega) and the online verification services of the cell banks Japanese Collection of Research Bioresources (JCRB) Cell Bank and DSMZ. Of note, a primary source genetic reference is not available for the cell lines OCI-LY3, OCI-LY4 and

OCI-LY7 (the original cell line stock in Ontario has not been maintained), however the intra-laboratory identity of these lines has been confirmed over time and the results of experiments using these cell lines are consistent with those previously reported (22).

BCR crosslinking

Cells (5×10^6 in 0.5 mL RPMI) were stimulated with 10 μg/ml goat anti-human IgM (Jackson ImmunoResearch Laboratories Inc., cat.# 309-006-043) or goat anti-human IgG (Jackson ImmunoResearch Laboratories Inc., cat.# 109-006-006) for 10 min (22, 28). The cells were either lysed and used for qualitative Western blotting or fixed in formalin and utilized for cell pellet microarray construction.

Cell lysis and immunoblotting

The cells were lysed in NP-40 containing buffer supplemented with protease and phosphatase inhibitors as described previously (22). Protein concentrations were assessed by Bradford assay (Bio-Rad Laboratories, Inc., Hercules, CA) and the samples were boiled for 3 min in 2x Laemmli sample buffer prior to loading onto a gel. Equal amounts of protein were separated by 4-15% sodium dodecyl sulfate-polyacrylamide gel electrophoresis (SDS-PAGE) (Bio-Rad Laboratories, Inc.) and transferred to Trans-Blot® supported nitrocellulose membrane (Bio-Rad Laboratories, Inc, Hercules, CA). Transferred proteins were visualized using Ponceau S staining (Sigma, St. Louis, MO) and examined for equal loading. Nitrocellulose was rinsed with Tris-buffered saline/0.1% Tween 20 (TBS-T) and blocked with 5% milk powder or 5% Fetal Bovine Serum (FBS) in TBS-T for 1 h at room temperature. Nitrocellulose membranes were then incubated with following antibodies: anti-phospho (pY396) LYN antibody in a 1:500 dilution (Epitomics, Inc., Burlingame, CA cat# 1645-1), 1:1000 anti-LYN (Cell Signaling Technology cat# 2796), 1:500 anti-phospho (pY323) SYK (Epitomics, Inc., cat# 2173-1), 1:1000 anti-SYK (Abcam, Cambridge, MA, cat# ab3113), 1:500 anti-phospho (pY223) BTK (Novus Biologicals, Inc., Littleton, CO, cat# NB100-92487) and 1:1000 anti-BTK antibody (Abcam, cat# ab54219), 1:500 (RXXS*/T*) anti-phospho AKT substrate (Cell Signaling Technology, cat# 9614), 1:1000 AKT1 antibody (Cell Signaling Technology, cat# 2938), anti-FOXO1 in 1:500 dilution (Cell Signaling, cat# 2880). To assess for equal loading, the blots were incubated with 1:500 anti-β-actin antibody (Santa Cruz Biotechnology, Inc., Santa Cruz, CA, cat.# sc-69879). The blots were stripped using Restore Plus Western Blot Stripping Buffer (Thermo Scientific, Rockford, IL, cat# 46430) and reprobed with a different antibody where indicated. After incubation with a primary antibody, the blots were washed four times for 15 min in TBS-T, followed by peroxidase conjugated goat anti-rabbit IgG (Thermo Scientific, Rockford, IL, cat.# 32460) or peroxidase conjugated goat anti-mouse IgG (Thermo Scientific, Rockford, IL, cat.# 32430) in a 1:500 dilution. Blots were then washed four times for 15 min in TBS-T, incubated with ECL chemiluminescent substrate according to manufacturer's instructions (Thermo Scientific, Rockford, IL, cat# 321), and exposed to autoradiography film (GE Healthcare, Buckinghamshire, UK).

Cell pellet microarrays

DLBCL cell lines, either untreated or crosslinked(22), were centrifuged in conical tubes for 5-10 min at 1000 rpm. The media was removed and the cells were washed once with

phosphate buffered saline (PBS). The cells were then pelleted by centrifugation and PBS was removed. The cell pellets were immediately resuspended in approximately 2 ml of 10% formalin and incubated at RT for 20 min. The formalin was removed and the cells were washed once with PBS, pelleted by centrifugation and resuspended in 1 ml PBS, transferred into 1.5 ml Eppendorf tube and stored at 4 °C. The cells were centrifuged for 10 min at 800 $\times g$ (2900 rpm) and the supernatant was removed. 50-60 μl of pre-warmed Histogel (Richard-Allan Scientific, Kalamazoo, MI) was added to each sample and the tubes were placed on ice to harden. The intact clots were then transferred to lens paper, placed in a histocassette, processed by standard methodologies overnight and embedded in paraffin within a single block to form a cell pellet microarray. The experiments for each cell line were performed at least in triplicate using independently treated cells.

Tissue microarray construction

Seventy four patients with DLBCL diagnosed between 2004 and 2009 were selected from the files of the Brigham and Women's Hospital (BWH, Table 1 and Supplementary Table S3) and one hundred and forty-eight patients with DLBCL diagnosed between 2000 and 2006 from Massachusetts General Hospital (MGH), respectively, with IRB approvals. Patients were classified according to the 2008 World Health Organization (WHO) classification. TMA construction was performed as described previously (29). Briefly, tissue cylinders with a diameter of 0.6 mm were punched from representative regions from each donor tissue block and brought into a recipient paraffin block using a semiautomatic robotic precision instrument. Three 0.6 mm cores of DLBCL were arrayed from each case.

Immunohistochemistry

Chromogenic and immunofluorescent immunohistochemistry was performed on DLBCL cell pellet microarrays and TMAs using 5 μm-thick sections on individual fresh-cut slides. We tested numerous anti-phospho-LYN, SYK and BTK antibodies under a wide range of conditions against untreated or sIg-crosslinked FFPE cell lines to identify the best reagent for IHC using FFPE tissue samples, comparing results by IHC to western blots of cell lysates under the same stimulation conditions and using the same antibodies. Based on this systematic approach we found the antibodies and procedures below gave optimal performance and reproducibility in qIF compared to others.

Slides were baked, soaked in xylene, passed through graded alcohols, and then pre-treated with either DAKO pH 9 retrieval solution (DAKO USA, Carpinteria, CA) for pLYN, pSYK and pBTK; 1 mM EDTA, pH 8 (Zymed, South San Francisco, CA) for FOXO1; 10 mM citrate, pH 6 for (RXXS*/T*) anti-phospho AKT substrate in a steam pressure cooker (Decloaking Chamber; BioCare Medical, Walnut Creek, CA) as per manufacturer's instructions followed by washing in distilled water. All further steps were done at room temperature in a hydrated chamber. Slides were then treated with peroxidase block (DAKO) for 5 min to quench endogenous peroxidase activity. Staining was performed with 1:600 anti-pY396 LYN, 1:100 anti-pY323 SYK, 1:25 anti-pY551 BTK (Epitomics, Inc., cat#1685-1), 1:100 anti-FOXO1, and 1:2500 (RXXS*/T*) anti-phospho AKT substrate antibodies for 1 h. Where indicated, double staining with CD20 antibody (clone L26; DAKO, ready to use solution) was performed. For immunofluorescent staining, slides were

washed in 50 mM Tris-HCl (pH 7.4) then labeled with diluted 1:200 Alexa 555 goat anti-rabbit (phosphomarkers, FOXO1) and Texas Red-conjugated goat anti-mouse (CD20) (Molecular Probes) for 30 min and coverslipped using ProlongGold antifade with DAPI (Molecular Probes). Immunoperoxidase staining was developed using a diaminobenzidine (DAB) chromogen kit (DAKO) per the manufacturer and counterstained with Harris hematoxylin (Polyscientific, Bay Shore, NY).

Quantification of immunofluorescence staining

The fluorescently stained slides were scanned using digital TissueFAXS™ imaging system and evaluated using TissueQuest™ imaging analysis software (Tissuegnostics Vienna, Austria). In brief, single cells were identified using an algorithm based on a preselected so-called master channel (based on nuclear DAPI staining) and the intensity of staining within either a cytoplasmic or total cell mask was quantified (Supplementary Figure S1 and S3). For cell line analysis the mean staining intensity of the phospho-markers (pLYN, pSYK, pBTK, pAKT-substrate) and FOXO1 was plotted against mean DAPI intensity. For the TMA analysis, the slides were double stained with a pan B cell marker CD20 along with either pLYN, pSYK, pBTK or FOXO1 and the mean intensity of a phospho-marker/FOXO1 staining was plotted against mean intensity of CD20 to determine the percentage of double positive cells. Positive cells were selected based on the cutoff values that were set by engaging negative controls and the backward and forward gating tool of the software. The results of the analysis are depicted in scattergrams (dot-plots) similar to those used in flow cytometry.

Statistical Analysis

A combined score for $\%pSYK^+$ and $\%pBTK^+$ was derived from linear regression using a maximum-likelihood algorithm(30) using the formula $\langle pSYK,pBTK\rangle = (pSYK_i + m pBTK_i)/(1 + m)$ where m is the slope of the fitted line and $\langle pSYK,pBTK\rangle$ has a range of 0–100. Estimates of statistical significance were based on the 2-tailed student t-test for continuous variables or the binomial distribution for discrete categories. For analysis of FOXO1 localization, the FOXO1 score $F_{cyt}=100\times FOXO1_{cyt}^+/FOXO1_{tot}^+$ was used, being the percent ratio of $FOXO1^+$ cells using either a cytoplasmic ($FOXO1_{cyt}$) or total cell ($FOXO1_{tot}$) mask.

For the analysis of TMA data a series of selection criteria were applied for inclusion of the specimen in the total sample (i) $CD20^+$>10% and >5% double positives for any core, (ii) where three cores were analyzable, reject those>40% different from the other two, (iii) two of three cores, subject to these exclusions, analyzable by Tissuequest™ for each of pLYN, pSYK-pBTK (paired), and FOXO1. Of 74 specimens within the BWH array, 60 fulfilled all criteria and are included in the final analysis. A validation TMA consisting of 148 cases was analyzed by the same selection criteria; 94 fulfilled all criteria and were included in final analysis. Further details and data tables are provided as Supplementary Information.

Results

Immunohistochemical signature for active BCR signaling in DLBCL cell lines

A panel of phospho-specific antibodies was developed to detect active BCR signaling by immunofluorescence of previously characterized DLBCL cell lines embedded in a cell pellet microarray. BCR activation was stimulated by crosslinking sIg with anti-immunoglobulin antibodies prior to fixation. We selected three phospho-specific antibodies directed toward known markers of BCR activation, LYN pY396 (pLYN) (31, 32), SYK pY323 (pSYK) (33, 34) and BTK pY551 (pBTK) (35, 36). Results for cell lines LY7, DHL4, LY3 and Toledo are shown (Figure 1A). Crosslinking of sIg led to a significant coordinate increase in phosphorylation of LYN, SYK and BTK over baseline levels in LY7, DHL4 and LY3 but not in Toledo. Similar results were obtained by chromogenic staining (Supplementary Figure S1).

Quantitative analysis of pLYN, pSYK and pBTK levels was performed using the TissueFAXS imaging system and Tissuequest™ software (Supplementary Figure S2 and Supplementary Methods). The percent positive cells $\%pLYN^+$, $\%pSYK^+$ and $\%pBTK^+$ (Figure 1B) agreed qualitatively with independent visual assessment by two expert pathologists (data not shown); qualitative Western blotting supports the effect of crosslinking (Supplementary Figure S3). In subsequent analysis we use the percent positive cells as independent variables (i.e. $pLYN=\%pLYN^+$, $pSYK=\%pSYK^+$, $pBTK=\%pBTK^+$).

qIF analysis of DLBCL cell lines reveals a metric for BCR activation

We next analyzed the percentage of $pLYN^+$, $pSYK^+$ and $pBTK^+$ cells from three independent experiments in a panel of ten cell lines. To assess the diagnostic potential of pLYN, pSYK and pBTK we compared the difference between mean values of the three phosphomarkers for untreated and crosslinked samples in each cell line (Supplementary Table S1). Although pLYN had the highest levels upon crosslinking, intermediate levels were also observed in 50% of untreated samples (DHL4, DHL6, HBL-1, LY3 and Pfeiffer). In contrast, pSYK and pBTK had very low or undetectable levels in all untreated samples that increased significantly upon crosslinking- and therefore better predictors of sIg mediated BCR activation than pLYN.

Of the three phosphomarkers pSYK is the strongest single predictor of BCR crosslinking. Five of ten cell lines (LY7, U2932, DHL4, DHL6, HBL-1) displayed pSYK<10 in uncrosslinked specimens and pSYK>50 in crosslinked specimens and a significant difference between the average values ($p \leq 0.06$, Supplementary Table S1, Figure 2A). These cell lines, referred to as Group I, comprise three BCR/GCB type (LY7, DHL4, DHL6) and two ABC type (U2932, HBL-1) cell lines according to previous molecular profiling studies, while of the other five cell lines, referred to as Group II, four are of the OxPhos type (Pfeiffer, Toledo, K422, LY4) cell lines (Supplementary Table S2). Group II included one BCR/ABC type cell line (LY3), for which the increase upon crosslinking was statistically significant for pLYN but did not reach statistical significance for pSYK or pBTK by qIF (pSYK untreated 0.8±0.7, crosslinked 7.8±4.9, $p=0.13$). Overall Group I showed high levels for all three phosphomarkers upon crosslinking, while Group II had negligible or more

variable levels of the three phosphomarkers upon crosslinking; only Group I cell lines showed a significant increase in at least two of the three phosphomarkers studied following BCR crosslinking. These results largely, but not completely, recapitulate changes in phosphomarkers observed by Western blotting as previously reported (22).

As pSYK and pBTK are well correlated (Figure 2B) we derived a weighted average ⟨pSYK,pBTK⟩ (see Supplementary Methods) and compared the average value for Group I crosslinked and untreated samples (Figure 2C). Both pSYK and ⟨pSYK,pBTK⟩ discriminate crosslinked from untreated samples with high statistical significance. Thus we selected ⟨pSYK,pBTK⟩ as a criterion of BCR activation incorporating two independent test of BCR signaling. A value of ⟨pSYK,pBTK⟩≥15 should be a strong indicator of proximal BCR pathway activation (BCR^+) in DLBCLs for which Group I cell lines are appropriate models. All untreated samples as well all crosslinked Group II cell lines except Pfeiffer are $\langle pSYK,pBTK\rangle^-$ (BCR^-) indicating undetectable proximal BCR pathway activation by qIF using this criterion.

Plotting ⟨pSYK,pBTK⟩ vs. pLYN for all samples in Group I (Figure 2D) we further noted that all samples with ⟨pSYK,pBTK⟩>15 also had pLYN>15, consistent with the hypothesis that phosphorylation of LYN is necessary but not sufficient for the phosphorylation of SYK and BTK (pLYN=74±13 for crosslinked Group I). Hence ⟨pSYK,pBTK⟩>15, pLYN>15 are appropriate criteria for detecting proximal BCR pathway activation in DLBCLs without falsely identifying BCR activation in any DLBCLs for which the cell line panel is representative.

qIF analysis of BCR signaling in a patient DLBCL tissue microarray

We proceeded to analyze pLYN, pSYK and pBTK levels by qIF in a tissue microarray (TMA) composed of 3 cores each from 60 primary DLBCL patient specimens. Aggregate clinical statistics are provided in Table 1 and summaries of all cases in Supplementary Table S3. In contrast to DLBCL cell lines, specimens in the TMA contain additional cell types. Therefore each phosphomarker was probed alongside the B cell-specific marker CD20, and the percent double positives recorded (pLYN=%$pLYN^+CD20^+$, pSYK=%$pSYK^+CD20^+$, pBTK=%$pBTK^+CD20^+$).

The %$CD20^+$ cells across the TMA was high (73±27%) and was highly correlated for each core between different slides (Δ(%$CD20^+$)=5±4%). Visual inspection confirmed that the vast majority (>90%) of $CD20^+$ cells are large in size with variably pleomorphic nuclei consistent with lymphoma. Results for all specimens are reported in Supplementary Table S4. The standard deviation between cores of the same specimen gives some measure of spatial heterogeneity within patient samples. The average error was 7.9%, 7.4% and 7.7% for pLYN, pSYK and pBTK, respectively. Excluding samples with average less than the average error, the relative error ($\Delta Z/Z$) was 31%, 45% and 40% for pLYN, pSYK and pBTK, respectively. Levels of pBTK vs. pSYK were higher in the primary DLBCL TMA than the cell pellet microarray (m_{TMA}=0.895, Figure 3 inset). Hence, the criterion ⟨pSYK,pBTK⟩=15 derived from cell pellet microarray was renormalized to ⟨pSYK,pBTK⟩=14.2 in the primary DLBCL TMA (see Supplementary Methods). The value of ⟨pSYK,pBTK⟩ vs. pLYN were plotted (Figure 3) and cases evaluated by the criteria ⟨pSYK,pBTK⟩=14.2, pLYN=15.

Almost half the cases (27/60, 45%) are $\langle pSYK,pBTK\rangle^{+}pLYN^{+}$, or BCR^{+}. Hence almost half the primary DLBCL cases examined had levels of phosphorylated BCR kinases consistent with proximal BCR pathway activation. Representative fields-of-view (FOVs) for the three phosphomarkers for two typical BCR^{+} cases (Figure 3, right) reveal a punctate membrane pattern for pLYN, pSYK and pBTK suggestive of BCR clustering at the cell surface. Similar findings were recently observed in ABC-type primary DLBCLs (21). Conversely, almost one quarter of cases (14/60, 23%) matched the criteria $\langle pSYK,pBTK\rangle^{-}pLYN^{-}$, or BCR^{-}. Visual assessment of these cases (Figure 3, lower left) confirmed these cases as true staining negatives. Results of chromogenic staining were in qualitative agreement with immunofluorescent analysis (Supplementary Figure S4), however CD20 cannot be simultaneously analyzed by this method of detection.

One quarter of cases (15/60, 25%) matched the criteria $\langle pSYK,pBTK\rangle^{-}pLYN^{+}$. The pLYN staining pattern for several such cases was similar to BCR^{+} specimens (Figure 3, bottom). These cases may represent false negatives according to $\langle pSYK,pBTK\rangle$, or either low (basal) or inactive BCR signaling consistent with certain untreated Group I cell lines (Figure 2A). A small group of cases (4/60, 7%) matched the criteria $\langle pSYK,pBTK\rangle^{+}pLYN^{-}$. Such cases are not observed in DLBCL cell lines nor are they consistent with the biological function of LYN upstream of SYK/BTK. Visual assessment revealed that pSYK staining was predominantly nuclear in several of these cases (Figure 3, top left). Nuclear localization of SYK has been previously described in B cells and squamous cell carcinoma and has been linked to alternate splicing and transcriptional repressor function (37-40). In the present context, however, such cases are inconsistent with the majority of $\langle pSYK,pBTK\rangle^{+}pLYN^{+}$ cases and were not designated positive for BCR signaling. The influence of nuclear pSYK staining was minimized by use of a cytoplasmic mask.

qIF analysis of BCR-mediated AKT activity and FOXO1 subcellular localization in DLBCL cell lines

Proximal BCR pathway activation in DLBCL TMA specimens cannot be controlled by manipulation of sIg as for the crosslinked samples in the DLBCL cell pellet microarray. Also, unlike the cell pellet microarray, patient samples are subject to numerous pre-analytical variables, notably time to fixation, that may significantly impact the detection of phosphoepitopes (41). Thus we extended our analysis on primary tissues to BCR-mediated downstream signaling molecules (15, 42) to further validate our assignment of cases as BCR^{+} and BCR^{-} and to demonstrate the detection of a complete signal transduction network in individual patient specimens. AKT phosphorylation is difficult to accurately assess in clinical specimens due to rapid antigen degradation by dephosphorylation (41, 43, 44). BCR-mediated activation of AKT however, promotes the phosphorylation of FOXO1 and its translocation from the nucleus to the cytoplasm; hence we anticipated that BCR^{+} DLBCLs would have a significantly higher proportion of cytoplasmic FOXO1 than BCR^{-} cases. Therefore we analyzed the DLBCL cell line panel for FOXO1. To quantitatively assess the degree of FOXO1 cytoplasmic localization, we defined a FOXO1 score $F_{cyt}=100\times FOXO1_{cyt}{}^{+}/FOXO1_{tot}{}^{+}$, being the percent ratio of $FOXO1^{+}$ cells using either a total cell ($FOXO1_{tot}$) or cytoplasmic ($FOXO1_{cyt}$) mask (Supplementary Figure S5 and Supplementary Methods).

Results for IHC of three representative cell lines (U2932, DHL6 and Toledo) are shown and correlated with qIF analysis of percent positive cells for FOXO1 using a cytoplasmic mask (Figure 4A). U2932 had low basal levels of $FOXO1_{cyt}^{+}$ and a significant increase upon crosslinking sIg, DHL6 had high basal levels and only a minor increase upon stimulation, while Toledo had constitutively high $FOXO1_{cyt}^{+}$ and no significant increase upon stimulation. Chromogenic staining was in qualitative agreement with immunoflourescent analysis (Supplementary Figure S6A) but quantitative delineation of the cytoplasm and extent of cytoplasmic localization was not possible by this detection method. In analysis of three independent experiments for all DLBCL cell lines, U2932 and HBL1 showed highly significant cytoplasmic localization of FOXO1 upon crosslinking, but the remaining DLBCL cell lines had constitutive cytoplasmic localization and increases upon crosslinking were not statistically significant (Supplementary Table S5, Supplementary Figure S7C).

Constitutive FOXO1 cytoplasmic localization may be either selected for or induced by the conditions of *in vitro* cell culture, yet FOXO1 localization may still be well correlated with AKT activation. We therefore assessed the level of AKT activation in the DLBCL panel using a phospho-specific AKT substrate antibody ($pAKT_{sub}$) that detects both autophosphorylated AKT and phosphorylated AKT substrates. Qualitative Western blotting (Figure 4B) supports the detection of autophosphorylated AKT by $pAKT_{sub}$ and qIF analysis (Supplementary Figure S7A) confirmed increased AKT activity upon crosslinking. Analysis of three independent experiments for all DLBCL cell lines revealed a statistically significant increase in $\%pAKT_{sub}^{+}$ cells for most cell lines (Supplementary Table S5, Supplementary Figure S7C). However $pAKT_{sub}^{+}$ levels did not correlate with BCR phosphomarkers across the panel, reflecting a degree of independence between the BCR and PI3K/AKT pathways in the cell lines. Nevertheless, changes in $pAKT_{sub}$ and FOXO1 cytoplasmic localization were correlated as evidenced by plotting the difference between crosslinked and untreated samples for the FOXO1 score (ΔF_{cyt}) vs. $pAKT_{sub}$ ($\Delta pAKT_{sub}$) for all cell lines in the panel (Pearson r=0.93, Figure 4C, Supplementary Figure S7C). Hence FOXO1 cytoplasmic localization is a valid surrogate marker of AKT activation in DLBCL.

Correlation of BCR signaling and FOXO1 localization in a patient DLBCL tissue microarray

Based on the correlation between AKT activity and FOXO1 localization, we proceeded to analyze the patient DLBCL TMA with FOXO1 and CD20 antibodies. The percent double positives, $\%FOXO1^{+}CD20^{+}$, was determined using both a total cell and cytoplasmic mask and the FOXO1 score (F_{cyt}) calculated as for the DLBCL cell lines. Use of the F_{cyt} score was validated by comparison of calculated F_{cyt} values for each case with visual scoring performed independently by two expert pathologists using (i) fluorescent staining and a 3-tier scoring system and (ii) chromogenic (DAB) staining and a 4-tier scoring system (Supplementary Figure S8). Mean F_{cyt} scores correlated quantitatively with both expert assessments.

The FOXO1 scores F_{cyt} for all 60 primary DLBCL patient specimens were compared with their previous evaluation of BCR signaling (Supplementary Table S4, Supplementary Figure S9). A representative $BCR^{-}F_{cyt}^{-}$ and $BCR^{+}F_{cyt}^{+}$ case are shown and correlated with qIF analysis of percent positive cells for FOXO1 using both cytoplasmic and whole cell masks

(Figure 5A). To test our criteria for active BCR signaling we compared the distribution of F_{cyt} values for $\langle pSYK,pBTK\rangle^{-}pLYN^{-}$ (BCR^{-}) and $\langle pSYK,pBTK\rangle^{+}pLYN^{+}$ (BCR^{+}) cases (Figure 5B). The mean F_{cyt} score for BCR^{+} cases was significantly higher than for BCR^{-} cases (57±32 vs. 28±25, p=0.004). No statistically significant difference in F_{cyt} score was observed for $\langle pSYK,pBTK\rangle^{+}pLYN^{-}$ and $\langle pSYK,pBTK\rangle^{-}pLYN^{+}$ subsets compared with BCR^{+} cases.

Analysis of Clinical Correlates

We compared our qIF analysis for pLYN, $\langle pSYK,pBTK\rangle$ and F_{cyt} to clinical data available for 60 patient specimens. There was no correlation between qIF variables and patient age, tumor location, or MIB proliferation index. A significant correlation was noted on the basis of sex however; females had higher values of $\langle pSYK,pBTK\rangle$ than males (35±29 vs. 18±23; p=0.01. Two thirds of BCR^{+} cases (18/27, 67%) were female compared to almost equal ratios for all specimens (32/60, 53%).

According to the COO profiling system ABC type tumors have significantly decreased survival versus GCB type tumors (45), and a significant number of ABC type DLBCLs are reported to rely on “chronic active” BCR signaling to mediate survival(21). Similarly, the CC profiling system identifies a subset of BCR type tumors that are reported to rely on tonic BCR signaling for survival (22, 23). We therefore analyzed staining by CD10, BCL6 and MUM1 and applied the algorithm of Hans et al. to all 60 cases (46). Overall 35 cases were assigned “GCB” and 25 “non-GCB”. We found no difference between any qIF variable for GCB vs. non-GCB specimens over all cases, nor any significant enrichment in GCB or non-GCB cases in the subset of BCR^{+} or BCR^{-} cases from the overall distribution (Supplementary Tables 3, 4).

Independent cohort validation

To confirm that our qIF analysis is not biased by patient selection or sample preparation procedures specific to one institution (BWH), we repeated our analysis on a validation TMA of cases selected and prepared independently (MGH). Of 145 primary DLBCL specimens on the MGH TMA, 94 passed all selection criteria and were analyzed as above. Aggregate statistics for CD20, pLYN, pSYK and pBTK were comparable between the two TMAs. The correlation between pSYK and pBTK on the MGH TMA was similar to the BWH TMA (Figure 6A, m=1.01), yielding the same normalized criteria of $\langle pSYK,pBTK\rangle$=14.2, pLYN=15. Almost half (44/94, 47%) of cases matched the criteria $\langle pSYK,pBTK\rangle^{+}pLYN^{+}$, or BCR^{+}, while one third of cases (33/94, 35%) matched the criteria $\langle pSYK,pBTK\rangle^{-}pLYN^{-}$, or BCR^{-} (Figure 6B). One eighth of cases (12/94, 13%) matched the criteria $\langle pSYK,pBTK\rangle^{-}pLYN^{+}$ and only a small number of cases (5/94, 5%) matched the criteria $\langle pSYK,pBTK\rangle^{+}pLYN^{-}$.

The difference between the mean F_{cyt} score for BCR^{+} and BCR^{-} cases in the MGH TMA was highly significant (70±25 vs. 34±23, $p<10^{-8}$, Figure 6C). We further analyzed staining by CD10, BCL6 and MUM1 and applied the algorithm of Hans et al. to all 94 cases (46). Equal numbers (47 cases each) were assigned “GCB” and “non-GCB”. We found no difference between any phosphomarker for GCB vs. non-GCB specimens over all 94 patient

specimens nor any significant variation in GCB or non-GCB cases in the subset of BCR^+ or BCR^- cases from the overall distribution, although GCB cases had a higher average value of F_{cyt} than non-GCB cases (61±29 vs. 44±28, p=0.008). In summary, our analysis of an independent cohort validates the results of our qIF analysis, with a similar distribution of cases, a clear correlation between BCR^+ cases and increased F_{cyt} values, and lack of correlation between qIF analysis of BCR phosphomarkers and IHC-based molecular profiling.

Discussion

This study establishes the use of qIF to identify proximal BCR activation in FFPE biopsy samples of DLBCL. From quantitative analysis of the phosphorylated kinases LYN, SYK and BTK and the weighted average ⟨pSYK,pBTK⟩ we developed and validated criteria for identifying proximal BCR signaling in DLBCL cell lines. When applied to two independent patient TMAs, this analysis revealed that almost half of patient specimens exhibit a signature of proximal BCR signaling (BCR^+) *in situ*. We also found that proximal BCR signaling correlates with increased cytoplasmic localization of the pro-survival transcription factor FOXO1, further suggesting a key role for BCR signaling in the activation of the PI3K/AKT/FOXO1 survival pathway *in vivo*. Surprisingly, we found no correlation between our qIF analysis of BCR signaling and IHC-based molecular profiling by the Hans' algorithm. We note however, that a similar lack of correlation was observed in a separate, recent study (24).

A major concern with phospho-specific epitopes in primary patient specimens is the influence of pre-analytical variables, especially the time to fixation that is uncontrolled in a retrospective analysis of paraffin-embedded specimens. Preliminary results on the spleens of mice following the introduction of DLBCL xenografts (LY1 cell line, data not shown) suggest that BCR phosphomarkers used in this study remain detectable by chromogenic staining following at least 30 minutes delay prior to fixation. Previous studies determined the half-life of FOXO1 to be at least one hour in HepG2 and HEK293T cells (47, 48). The similarity of our results on TMAs from two separate institutions suggests that errors arising from pre-analytical variables will not significantly distort qIF analysis of BCR signaling in multi-center studies. Separate institutions may use common procedures giving rise to the same systematic error however, so prospective studies of pre-analytic variables in the context of primary human specimens utilizing similar detection protocols as described here are required to validate the qIF method. Notwithstanding these limitations however, our results reveal that at minimum, approximately one-half of primary patient specimens contain detectable levels of pLYN, pSYK, pBTK and FOXO1 even in the absence of stringent pre-analytical protocols.

Although activation of the BCR signaling cascade is a common feature of DLBCL *in situ*, we emphasize that the biological significance of these results still needs to be confirmed. Of note, we observed increased levels of pSYK and pBTK following crosslinking sIg in the GCB cell lines DHL4 and DHL6. While in agreement with previous results from Western blotting of these cell lines following stimulation (22), and evidence that DHL4 and DHL6 are sensitive to chemical inhibitors of SYK (22, 24), DHL4 and DHL6 are unaffected by shRNA-mediated knockdown of CD79 or SYK(21), implying that these lines do not rely on

"chronic active" BCR signaling for survival. Thus it is likely that the detection of an inducible BCR signaling cascade is necessary but not sufficient for determining if a cell line requires BCR signaling for survival in the absence of functional data. Similarly, determining whether qIF analysis can serve to predict if an individual patient's tumor is dependent on BCR signaling for growth and survival will require a detailed study that correlates the BCR score with clinical responses in trials using BCR-targeted therapies.

Our analysis of DLBCL cell lines further revealed a significant correlation between sIg crosslinking and BCR-associated activation of kinases LYN, SYK and BTK, and between the change in AKT activation and the change in cytoplasmic FOXO1 localization, but only a weak, direct correlation between BCR and AKT signaling. This suggests that AKT may be activated in these cell lines through BCR-independent mechanisms such as PTEN deletions, mutations in PI3K subunits or amplification of AKT (19, 49, 50). Similarly, while we observed a higher degree of cytoplasmic localization of FOXO1 among BCR^+ than among BCR^- primary tumors, supporting the notion that BCR and AKT signaling are linked in DLBCL, exceptions among individual cases were not infrequent (Supplementary Table S4). Possible explanations include that, in a subset of cases, active BCR signaling does not fully translate to AKT activation, and conversely that, in a subset of cases, constitutive activation of the PI3K/AKT pathway occurs independently of proximal BCR activation. Similar to the validation of the BCR^+ signature, a deternination of the diagnostic utility of the F_{cyt} score in primary tumors will require studies correlating qIF analysis with clinical response in trials using directed therapies.

An unanticipated finding of our study was the detection of pLYN without detection of pSYK or pBTK in unstimulated GCB cell lines DHL4 and DHL6 and in 12-25% of primary DLBCL specimens. This precludes the use of pLYN as a primary criterion for BCR-specific signaling, although it is a useful secondary criterion, i.e. pLYN is necessary but not sufficient for a tumor to be classified as BCR^+. The unique dual role of LYN in B cells beyond the activation of SYK and BTK is well documented, including negative regulatory roles in BCR signaling via phosphorylation of ITIMS in CD22, CD72, PIR-B and FcyRIIB (51, 52). Consistent with the notion that LYN has additional roles in tumor cell survival, the GCB cell lines OCI-Ly7 and OCI-Ly19, which were resistant to BTK shRNAs, were sensitive to one of three LYN shRNAs (NM_002350_bp1462) tested by Davis et al. (21). The biological significance of LYN phosphorylation in DLBCL is a topic of future investigation.

We propose that the application of qIF represents a valuable new tool to complement molecular profiling studies and flow cytometry in the analysis of tumor-associated signaling pathways. In contrast to transcriptional profiling, qIF enables the analysis of post-translational modifications and subcellular localization of the expressed targets within a heterogeneous population of cells, which are not readily addressed by mRNA–based gene expression studies. While flow cytometry can be used to detect post-translational modifications and analyze heterogeneous cell populations, intracellular markers are technically demanding and abnormally large tumor cells may go undetected due to either cell loss during processing or a paucity of neoplastic cells. Allocation of appropriate material for flow cytometric studies can also pose a challenge since neoplastic infiltrates

may not involve the entire specimen and evaluation of the signaling molecules *in situ* using qIF offers an additional advantage. Finally, we demonstrate that qIF can successfully analyze the functional state of a signal transduction cascade in paraffin-embedded tissue, which is frequently the only patient material available for evaluation by the pathologist.

The use of qIF to analyze the functional state and localization of signaling components in routine clinical specimens is of great value for comparison with results obtained from model systems or cell lines. In this study alone three quantitative differences were observed between DLBCL cell lines and tissue specimens: (i) The level of pBTK relative to pSYK in tissue specimens was twice that observed in DLBCL cell lines, (ii) FOXO1 localization varied almost the entire range F_{cyt}=0-100 in tissue specimens, but was significantly cytoplasmic (F_{cyt}>50) in the majority of DLBCL cell lines, (iii) pLYN levels were highly correlated with FOXO1 cytoplasmic localization in tissue specimens suggesting it was a significant indicator of BCR signaling, whereas several unstimulated DLBCL cell lines had significant levels of pLYN suggesting it was a poor primary indicator of BCR signaling. This illustrates both the importance of validating molecular hypotheses based on model systems in primary tissue samples and the value of qIF analysis in performing such validation studies.

In addition to the BCR/PI3K/AKT pathways examined in this study, other survival pathways implicated in DLBCL include constitutive activation of NF-κB via B cell activation factor (BAFF)-R (BR3) (53), p38 activated protein kinase (MAPK) expression (54) or Hedgehog signaling pathways (55). Future qIF studies combining phospho-specific antibodies to critical signaling molecules in these additional signaling pathways could address their contribution to DLBCL biology *in situ*. Moreover, the development of qIF-based signatures for these and other components could provide a means of comprehensive analysis of the molecular basis of BCR-mediated signaling and survival in DLBCL tumors.

In conclusion, we have developed a tissue-based qIF approach for analyzing components of the proximal BCR and distal AKT/FOXO1 signaling pathways in formalin-fixed, paraffin-embedded tissue. Quantification of signaling proteins in tissue shall be of great value in identifying future therapeutic targets in DLBCL and other aggressive lymphomas and in correlating the therapeutic efficacy of inhibitors of the BCR and PI3K/AKT pathways. Moreover, qIF-based classification of DLBCL may aid in understanding of the basic differences in the biology of these tumors and their variable response to treatment. The technology and analytical approach presented here can be used as a basis for dissection of activity of signaling pathways in many different hematolymphoid and nonhematolymphoid malignancies.

Supplementary Material

Refer to Web version on PubMed Central for supplementary material.

Acknowledgements

We would like to thank Dr. Jon Aster, Donna Neuberg and Kristen Stevenson for critical review of the manuscript and useful discussions. We also thank Prof. Georg Lenz for kindly providing U2932 and HBL-1 cell lines. This

research was supported by the National Institutes of Health under Ruth L. Kirschstein National Research Service Award T32HL007627 from the National Heart, Lung and Blood Institute.

References

1. Armitage JO, Weisenburger DD. New approach to classifying non-Hodgkin's lymphomas: clinical features of the major histologic subtypes. Non-Hodgkin's Lymphoma Classification Project. J Clin Oncol. 1998; 16:2780–95. [PubMed: 9704731]
2. Hunt KE, Reichard KK. Diffuse large B-cell lymphoma. Arch Pathol Lab Med. 2008; 132:118–24. [PubMed: 18181663]
3. Abramson JS, Shipp MA. Advances in the biology and therapy of diffuse large B-cell lymphoma: moving toward a molecularly targeted approach. Blood. 2005; 106:1164–74. [PubMed: 15855278]
4. Coiffier B. Rituximab therapy in malignant lymphoma. Oncogene. 2007; 26:3603–13. [PubMed: 17530014]
5. Lam K-P, Kühn R, Rajewsky K. In vivo ablation of surface immunoglobulin on mature B cells by inducible gene targeting results in rapid cell death. Cell. 1997; 90:1073–83. [PubMed: 9323135]
6. Chan WC. Pathogenesis of diffuse large B cell lymphoma. Int J Hematol. 2010; 92:219–30. [PubMed: 20582737]
7. Witzig TE, Gupta M. Signal transduction inhibitor therapy for lymphoma. Hematology Am Soc Hematol Educ Program. 2010; 2010:265–70. [PubMed: 21239804]
8. Rajewsky K, Kanzler H, Hansmann M-L, Küppers R. Normal and malignant B-cell development with special reference to Hodgkin's disease. Ann Oncol. 1997; 8(Suppl 2):79–81.
9. Kraus M, Alimzhanov MB, Rajewsky N, Rajewsky K. Survival of resting mature B lymphocytes depends on BCR signaling via the Igalpha/beta heterodimer. Cell. 2004; 117:787–800. [PubMed: 15186779]
10. Dal Porto JM, Gauld SB, Merrell KT, Mills D, Pugh-Bernard AE, Cambier J. B cell antigen receptor signaling 101. Mol Immunol. 2004; 41:599–613. [PubMed: 15219998]
11. Saouaf SJ, Mahajan S, Rowley RB, Kut SA, Fargnoli J, Burkhardt AL, et al. Temporal differences in the activation of three classes of non-transmembrane protein tyrosine kinases following B-cell antigen receptor surface engagement. Proc Natl Acad Sci USA. 1994; 91:9524–8. [PubMed: 7524079]
12. Cheng AM, Rowley B, Pao W, Hayday A, Bolen JB, Pawson T. Syk tyrosine kinase required for mouse viability and B-cell development. Nature. 1995; 378:303–6. [PubMed: 7477353]
13. Cornall RJ, Cheng AM, Pawson T, Goodnow CC. Role of Syk in B-cell development and antigen-receptor signaling. Proc Natl Acad Sci USA. 2000; 97:1713–8. [PubMed: 10677523]
14. Turner M, Mee PJ, Costello PS, Williams O, Price AA, Duddy LP, et al. Perinatal lethality and blocked B-cell development in mice lacking the tyrosine kinase Syk. Nature. 1995; 378:298–302. [PubMed: 7477352]
15. Gold MR, Scheid MP, Santos L, Dang-Lawson M, Roth RA, Matsuuchi L, et al. The B cell antigen receptor activates the Akt (protein kinase B)/glycogen synthase kinase-3 signaling pathway via phosphatidylinositol 3-kinase. J Immunol. 1999; 163:1894–905. [PubMed: 10438924]
16. Aagaard-Tillery KM, Jelinek DF. Phosphatidylinositol 3-kinase activation in normal human B lymphocytes. J Immunol. 1996; 156:4543–54. [PubMed: 8648095]
17. Brunet A, Bonni A, Zigmond MJ, Lin MZ, Juo P, Hu LS, et al. Akt promotes cell survival by phosphorylating and inhibiting a Forkhead transcription factor. Cell. 1999; 96:857–68. [PubMed: 10102273]
18. Maiese K, Chong ZZ, Shang YC, Hou J. A “FOXO” in sight: targeting Foxo proteins from conception to cancer. Med Res Rev. 2009; 29:395–418. [PubMed: 18985696]
19. Fillmore GC, Wang Q, Carey MJ, Kim C-H, Elenitoba-Johnson KSJ, Lim MS. Expression of Akt (protein kinase B) and its isoforms in malignant lymphomas. Leuk Lymphoma. 2005; 46:1765–73. [PubMed: 16263580]
20. Lenz G, Staudt LM. Aggressive lymphomas. N Engl J Med. 2010; 362:1417–29. [PubMed: 20393178]

21. Davis RE, Ngo VN, Lenz G, Tolar P, Young RM, Romesser PB, et al. Chronic active B-cell-receptor signalling in diffuse large B-cell lymphoma. Nature. 2010; 463:88–92. [PubMed: 20054396]
22. Chen L, Monti S, Juszczynski P, Daley J, Chen W, Witzig TE, et al. SYK-dependent tonic B-cell receptor signaling is a rational treatment target in diffuse large B-cell lymphoma. Blood. 2008; 111:2230–7. [PubMed: 18006696]
23. Monti S, Savage KJ, Kutok JL, Feuerhake F, Kurtin P, Mihm M, et al. Molecular profiling of diffuse large B-cell lymphoma identifies robust subtypes including one characterized by host inflammatory response. Blood. 2005; 105:1851–61. [PubMed: 15550490]
24. Cheng S, Coffey G, Zhang XH, Shaknovich R, Song Z, Lu P, et al. SYK inhibition and response prediction in diffuse large B-cell lymphoma. Blood. 2011; 118:6342–52. [PubMed: 22025527]
25. Friedberg JW, Sharman J, Sweetenham J, Johnston PB, Vose JM, Lacasce A, et al. Inhibition of Syk with fostamatinib disodium has significant clinical activity in non-Hodgkin lymphoma and chronic lymphocytic leukemia. Blood. 2010; 115:2578–85. [PubMed: 19965662]
26. de Rooij MF, Kuil A, Geest CR, Eldering E, Chang BY, Buggy JJ, et al. The clinically active BTK inhibitor PCI-32765 targets B-cell receptor- and chemokine-controlled adhesion and migration in chronic lymphocytic leukemia. Blood. 2012; 119:2590–4. [PubMed: 22279054]
27. Hoellenriegel J, Meadows SA, Sivina M, Wierda WG, Kantarjian H, Keating MJ, et al. The phosphoinositide 3′-kinase delta inhibitor, CAL-101, inhibits B-cell receptor signaling and chemokine networks in chronic lymphocytic leukemia. Blood. 2011; 118:3603–12. [PubMed: 21803855]
28. Juszczynski P, Chen L, O'Donnell E, Polo JM, Ranuncolo SM, Dalla-Favera R, et al. BCL6 modulates tonic BCR signaling in diffuse large B-cell lymphomas by repressing the SYK phosphatase, PTPROt. Blood. 2009; 114:5315–21. [PubMed: 19855081]
29. Kononen J, Bubendorf L, Kallioniemi A, Barlund M, Schraml P, Leighton S, et al. Tissue microarrays for high-throughput molecular profiling of tumor specimens. Nat Med. 1998; 4:844–7. [PubMed: 9662379]
30. Ripley BD, Thompson M. Regression Techniques for the Detection of Analytical Bias. Analyst. 1987; 112:377–83.
31. Yamanashi Y, Kakiuchi T, Mizuguchi J, Yamamoto T, Toyoshima K. Association of B cell antigen receptor with protein tyrosine kinase Lyn. Science. 1991; 251:192–4. [PubMed: 1702903]
32. Burkhardt AL, Brunswick M, Bolen JB, Mond JJ. Anti-immunoglobulin stimulation of B lymphocytes activates src-related protein-tyrosine kinases. Proc Natl Acad Sci USA. 1991; 88:7410–4. [PubMed: 1714601]
33. Geahlen RL. Syk and pTyr'd: Signaling through the B cell antigen receptor. Biochim Biophys Acta. 2009; 1793:1115–27. [PubMed: 19306898]
34. Keshvara LM, Isaacson CC, Yankee TM, Sarac R, Harrison ML, Geahlen RL. Syk- and Lyn-dependent phosphorylation of Syk on multiple tyrosines following B cell activation includes a site that negatively regulates signaling. J Immunol. 1998; 161:5276–83. [PubMed: 9820500]
35. Rawlings DJ, Scharenberg AM, Park H, Wahl MI, Lin S, Kato RM, et al. Activation of BTK by a phosphorylation mechanism initiated by SRC family kinases. Science. 1996; 271:822–5. [PubMed: 8629002]
36. Nisitani S, Kato RM, Rawlings DJ, Witte ON, Wahl MI. In situ detection of activated Bruton's tyrosine kinase in the Ig signaling complex by phosphopeptide-specific monoclonal antibodies. Proc Natl Acad Sci USA. 1999; 96:2221–6. [PubMed: 10051622]
37. Zhou F, Hu J, Ma H, Harrison ML, Geahlen RL. Nucleocytoplasmic trafficking of the Syk protein tyrosine kinase. Mol Cell Biol. 2006; 26:3478–91. [PubMed: 16611990]
38. Luangdilok S, Box C, Patterson L, Court W, Harrington K, Pitkin L, et al. Syk tyrosine kinase is linked to cell motility and progression in squamous cell carcinomas of the head and neck. Cancer Res. 2007; 67:7907–16. [PubMed: 17699797]
39. Wang L, Duke L, Zhang PS, Arlinghaus RB, Symmans WF, Sahin A, et al. Alternative splicing disrupts a nuclear localization signal in spleen tyrosine kinase that is required for invasion suppression in breast cancer. Cancer Res. 2003; 63:4724–30. [PubMed: 12907655]

40. Pighi C, Gu T-L, Dalai I, Barbi S, Parolini C, Bertolaso A, et al. Phospho-proteomic analysis of mantle cell lymphoma cells suggests a pro-survival role of B-cell receptor signaling. Cell Oncol (Dordr). 2011; 34:141–53. [PubMed: 21394647]
41. Baker AF, Dragovich T, Ihle NT, Williams R, Fenoglio-Preiser C, Powis G. Stability of phosphoprotein as a biological marker of tumor signaling. Clin Cancer Res. 2005; 11:4338–40. [PubMed: 15958615]
42. Srinivasan L, Sasaki Y, Calado DP, Zhang B, Paik JH, DePinho RA, et al. PI3 kinase signals BCR-dependent mature B cell survival. Cell. 2009; 139:573–86. [PubMed: 19879843]
43. Bai Y, Tolles J, Cheng H, Siddiqui S, Gopinath A, Pectasides E, et al. Quantitative assessment shows loss of antigenic epitopes as a function of pre-analytic variables. Lab Invest. 2011; 91:1253–61. [PubMed: 21519325]
44. Pinhel IF, Macneill FA, Hills MJ, Salter J, Detre S, A'Hern R, et al. Extreme loss of immunoreactive p-Akt and p-Erk1/2 during routine fixation of primary breast cancer. Breast Cancer Res. 2010; 12:R76. [PubMed: 20920193]
45. Alizadeh AA, Eisen MB, Davis RE, Ma C, Lossos IS, Rosenwald A, et al. Distinct types of diffuse large B-cell lymphoma identified by gene expression profiling. Nature. 2000; 403:503–11. [PubMed: 10676951]
46. Hans CP, Weisenburger DD, Greiner TC, Gascoyne RD, Delabie J, Ott G, et al. Confirmation of the molecular classification of diffuse large B-cell lymphoma by immunohistochemistry using a tissue microarray. Blood. 2004; 103:275–82. [PubMed: 14504078]
47. Aoki M, Jiang H, Vogt PK. Proteasomal degradation of the FoxO1 transcriptional regulator in cells transformed by the P3k and Akt oncoproteins. Proc Natl Acad Sci U S A. 2004; 101:13613–7. [PubMed: 15342912]
48. Perrot V, Rechler MM. The coactivator p300 directly acetylates the forkhead transcription factor Foxo1 and stimulates Foxo1-induced transcription. Mol Endocrinol. 2005; 19:2283–98. [PubMed: 15890677]
49. Dahia PL, Aguiar RC, Alberta J, Kum JB, Caron S, Sill H, et al. PTEN is inversely correlated with the cell survival factor Akt/PKB and is inactivated via multiple mechanismsin haematological malignancies. Hum Mol Genet. 1999; 8:185–93. [PubMed: 9931326]
50. Vivanco I, Sawyers CL. The phosphatidylinositol 3-Kinase AKT pathway in human cancer. Nat Rev Cancer. 2002; 2:489–501. [PubMed: 12094235]
51. Ravetch JV, Lanier LL. Immune inhibitory receptors. Science. 2000; 290:84–9. [PubMed: 11021804]
52. Scapini P, Pereira S, Zhang H, Lowell CA. Multiple roles of Lyn kinase in myeloid cell signaling and function. Immunol Rev. 2009; 228:23–40. [PubMed: 19290919]
53. Pham LV, Fu L, Tamayo AT, Bueso-Ramos C, Drakos E, Vega F, et al. Constitutive BR3 receptor signaling in diffuse, large B-cell lymphomas stabilizes nuclear factor-kappaB-inducing kinase while activating both canonical and alternative nuclear factor-kappaB pathways. Blood. 2011; 117:200–10. [PubMed: 20889926]
54. Ding H, Gabali AM, Jenson SD, Lim MS, Elenitoba-Johnson KSJ. P38 mitogen activated protein kinase expression and regulation by interleukin-4 in human B cell non-Hodgkin lymphomas. J Hematop. 2009; 2:195–204. [PubMed: 20309428]
55. Singh RR, Kim JE, Davuluri Y, Drakos E, Cho-Vega JH, Amin HM, et al. Hedgehog signaling pathway is activated in diffuse large B-cell lymphoma and contributes to tumor cell survival and proliferation. Leukemia. 2010; 24:1025–36. [PubMed: 20200556]

Statement of Translational Relevance

Diffuse large B cell lymphoma (DLBCL) is the most common type of Non-Hodgkin lymphoma with a poor prognosis in approximately 50% of patients. New therapeutic approaches are focused on targeting specific signaling pathways using small molecule inhibitors. B cell receptor (BCR) mediated signaling is an important pathway in DLBCL pathogenesis. In this work we evaluated BCR signaling using quantitative immunofluorescence (qIF) in paraffin-embedded DLBCL specimens and identified a robust signature based on the quantitation of phosphorylated proximal BCR signaling kinases LYN, SYK and BTK. We detected active BCR signaling in almost 50% of patient tumors and found that this signaling translated into regulation of the pro-apoptotic transcription factor FOXO1. This study provides a foundation for dissection of signal transduction pathways in DLBCL and other malignancies using an immunostaining approach and implicates the use of qIF as a tool to identify patients with active BCR signaling that are receiving anti-BCR and other anti-tumor therapies.

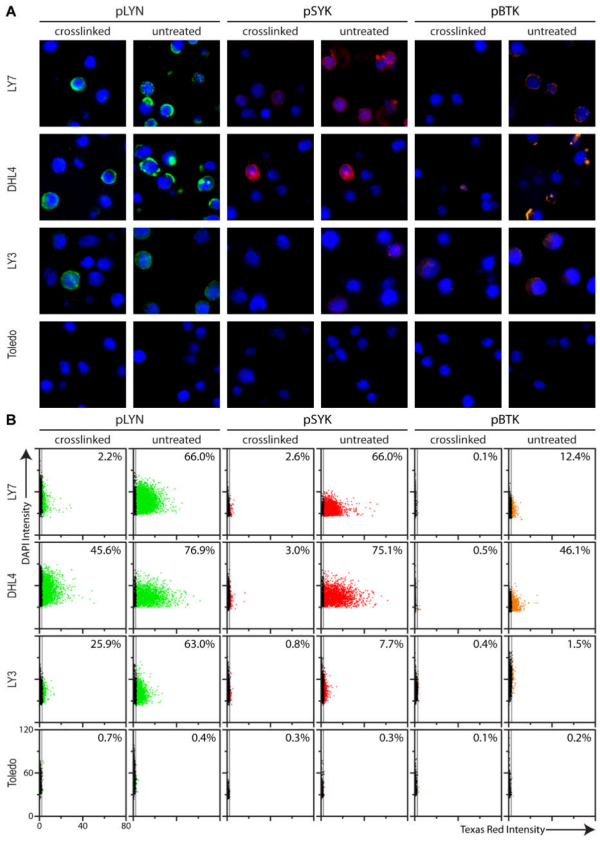

Figure 1. Quantitative immunofluorescence of proximal BCR signaling in DLBCL cell lines

(A) Immunofluorescent staining of paraffin-embedded DLBCL cell lines LY7, DHL4, LY3 and Toledo, untreated and BCR crosslinked, with anti-pLYN (Y396) (green), anti-pSYK (Y323) (red), and anti-pBTK (Y551) (orange). Nuclei stained with DAPI (blue). Increased phosphorylation upon crosslinking is observed for LY7, DHL4 and LY3. No significant phosphorylation is observed for Toledo in either untreated or crosslinked cells.

(B) Scatterplot of total intensity per cell for phosphomarkers (Texas Red) vs. nuclear intensity (DAPI) from Tissuequest™ analysis of cells shown in (A). The value displayed in the top right corner of each scatterplot is the % positive (average of three independent experiments). Quantitative analysis agrees well with qualitative visual assessment (Note: cells negative for staining lie along the y-axis of the scatterplot).

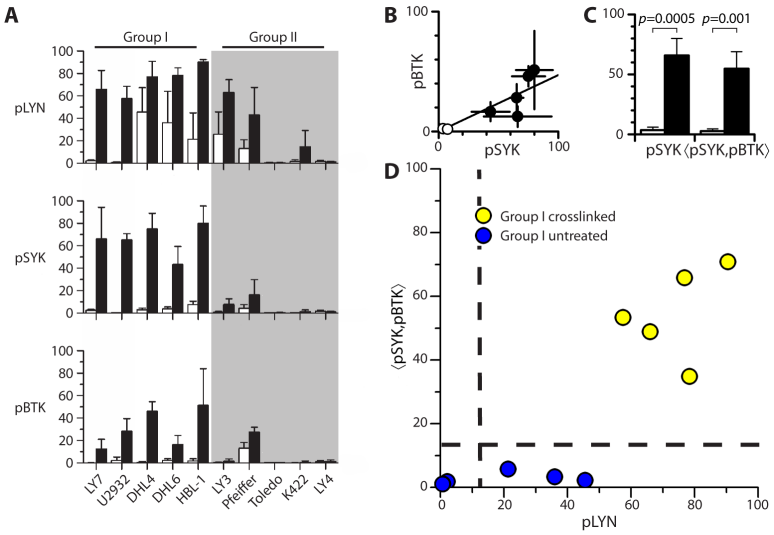

Figure 2. Analysis of phosphomarkers for active BCR signaling in DLBCL cell lines

(A) Histogram of %pLYN$^+$ (pLYN), %pSYK$^+$ (pSYK) and %pBTK$^+$ (pBTK) for qIF analysis of untreated (white) and crosslinked (black) samples in a panel of DLBCL cell lines. Cell lines are grouped according to similarity of response to crosslinking for all three phosphomarkers (average of three independent experiments).

(B) Scatterplot of pBTK vs pSYK for Group I cell lines and line of best fit.

(C) Mean pSYK and ⟨pSYK,pBTK⟩ for untreated (white) and crosslinked (black) Group I cell lines.

(D) Scatterplot of ⟨pSYK,pBTK⟩ vs. pLYN qIF data for Group I DLBCL cell lines. Horizontal dashed line represents criterion ⟨pSYK,pBTK⟩=15 distinguishing untreated and crosslinked samples. Vertical dashed line represents pLYN=15 as independent criterion for crosslinked samples.

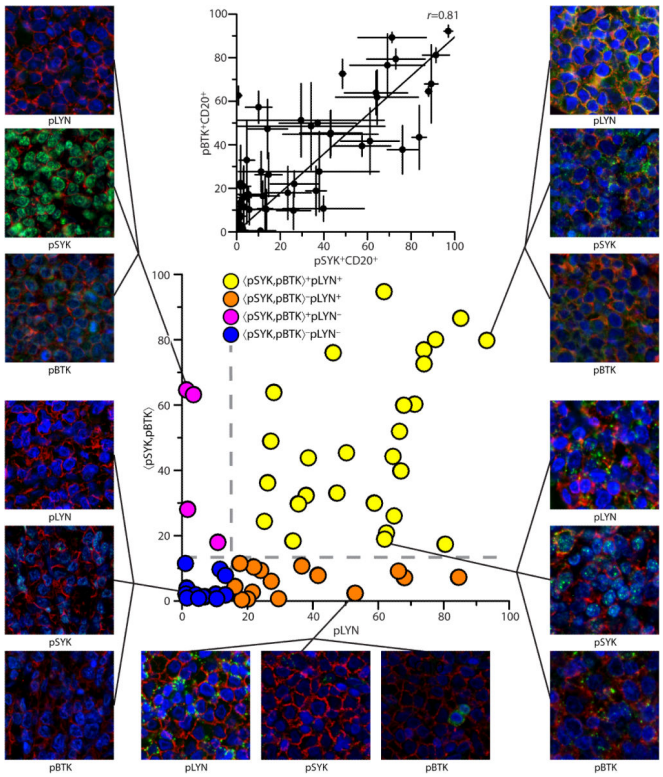

Figure 3. Quantitative assessment of active BCR signaling in primary DLBCL tumors

Scatterplot of ⟨pSYK,pBTK⟩ vs. pLYN for primary DLBCL patient specimens in a TMA analyzed by qIF for pLYN (Y396), pSYK (Y323) and pBTK (Y551) and CD20. Dashed lines represent criteria for active BCR signaling (⟨pSYK,pBTK⟩>14.2, pLYN>15). Specimens are categorized as ⟨pSYK,pBTK⟩$^{+}$pLYN^{+}=BCR^{+} (yellow), ⟨pSYK,pBTK⟩$^{-}$pLYN^{+}(orange), ⟨pSYK,pBTK⟩$^{+}$pLYN^{-}(magenta), or ⟨pSYK,pBTK⟩$^{-}$pLYN^{-}=BCR^{-}(*blue*). Representative fields of view for three BCR phosphomarkers (green) and CD20 (red) are shown for selected specimens, Clockwise from top right (i)strong BCR^{+}, (ii) intermediate BCR^{+}, (iii) ⟨pSYK,pBTK⟩$^{-}$pLYN^{+}, (iv) BCR^{-}, (v) ⟨pSYK,pBTK⟩$^{+}$pLYN^{-} (nuclear pSYK). (inset) Scatterplot of pBTK vs. pSYK for qIF analysis of DLBCL patient specimens, Pearson correlation coefficient r=0.81.

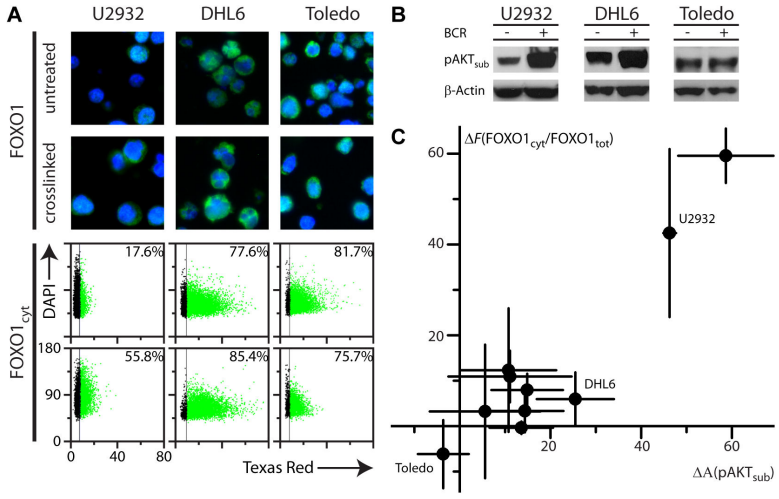

Figure 4. Analysis of FOXO1 cytoplasmic localization and AKT activity in DLBCL cell lines

(A) Top panels: Immunofluorescent staining of paraffin-embedded DLBCL cell lines U2932, DHL6 and Toledo, untreated and crosslinked, anti-FOXO1 (green). Untreated U2932 has little cytoplasmic FOXO1 with a significant increase upon crosslinking, Untreated DHL6 has significant cytoplasmic FOXO1 and only slight increase upon crosslinking, while untreated Toledo shows constitutively high levels of cytoplasmic FOXO1 that does not increase with crosslinking. Bottom panels: Scatterplots of staining intensity for FOXO1 (Texas Red) using a cytoplasmic mask vs. nuclear intensity (DAPI) from Tissuequest™ analysis per cell for the cell lines shown in the top panels. The percentage of positive cells displayed in the upper right corner of each scatterplot is the average of three independent experiments.

(B) Qualitative Western blotting with $pAKT_{sub}$ antibody detects autophosphorylated AKT in DLBCL cell lines U2932, DHL6 and Toledo, and a significant increase for U2932, DHL6 but not Toledo upon BCR crosslinking.

(C) Scatterplot of the difference upon crosslinking for the cytoplasmic FOXO1 score ΔF_{cyt} vs. qIF analysis of AKT activity $\Delta pAKT_{sub}$ for panel of 10 DLBCL cell lines (average of three independent experiments).

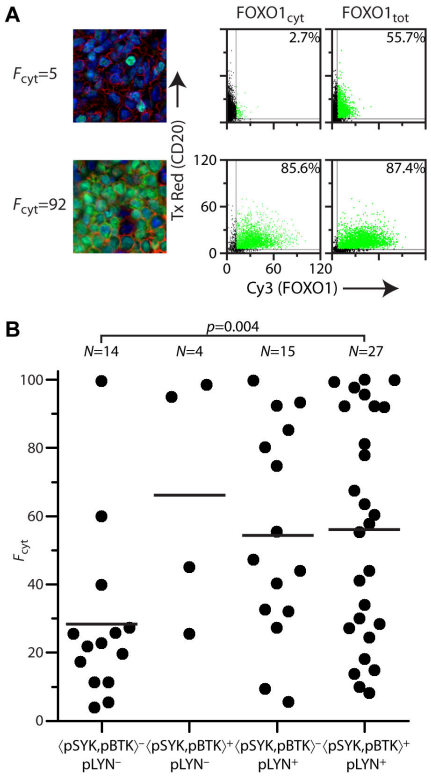

Figure 5. Quantitative assessment of FOXO1 cytoplasmic localization in primary DLBCL tumors

(A) Representative fields of view for BCR− (top row, left panel) and BCR+ (bottom row, left panel) primary DLBCL cases with low (Fcyt−) and high (Fcyt+) levels of cytoplasmic FOXO1, respectively. Scatterplots (right panels) of FOXO1 (Cy3) vs. CD20 (Texas Red) from Tissuequest{trade mark, serif} analysis of one core for each case, using either a cytoplasmic or whole cell mask for FOXO1. The Fcyt score for each core is calculated using the percent positive cells displayed in the upper right corners, the final Fcyt score for each case is the average of two or three analyzed cores. (B) Plot of individual Fcyt scores for cases in the DLBCL TMA: (−) arithmetic mean.

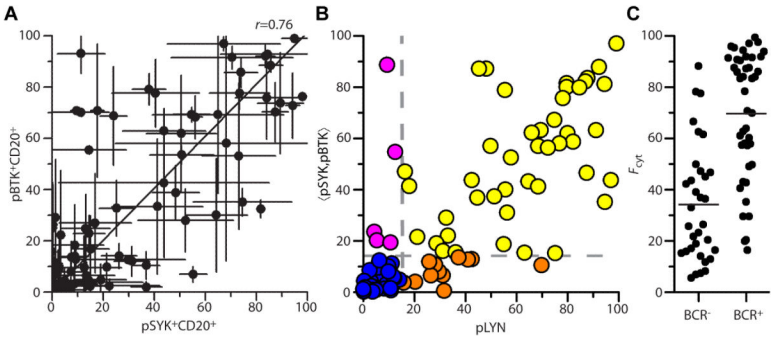

Figure 6. Validation of qIF in an independent cohort of primary DLBCL tumors

(A) Scatterplot of pBTK vs. pSYK for qIF analysis of MGH DLBCL TMA, Pearson correlation coefficient r=0.76.

(B) Scatterplot of ⟨pSYK,pBTK⟩ vs. pLYN for MGH DLBCL TMA analyzed by qIF for pLYN (Y396), pSYK (Y323) and pBTK (Y551) and CD20. Dashed lines represent criteria for active BCR signaling (⟨pSYK,pBTK⟩>14.2, pLYN>15). Specimens are categorized as $\langle pSYK,pBTK\rangle^{+}pLYN^{+}=BCR^{+}$ (yellow), $\langle pSYK,pBTK\rangle^{-}pLYN^{+}$(orange), $\langle pSYK,pBTK\rangle^{+}pLYN^{-}$(magenta), or $\langle pSYK,pBTK\rangle^{-}pLYN^{-}=BCR^{-}$(blue). (C) Plot of F_{cyt} scores (●) for BCR^{-} and BCR^{+} cases in the MGH DLBCL TMA: (—) arithmetic mean.

Table 1

Aggregate Clinical Statistics (BWH TMA)

No. cases		**60**
Age	Min.	27
	Med.	67
	Max.	87
Sex	Male	28
	Female	32
History	no h/o NHL:	51
	h/o of NHL:	9
Location	lymph node	29
	extra nodal	31
IHC profile:	GCB:	35
	Non-GCB	25